

## Grain Size Distribution and topological correlations During Ostwald Ripening: Monte Carlo Potts model simulation

Dr. Rifa J. El-Khozondar \*

Prof. Dr. Hala J. El-Khozondar \*\*

### الملخص

توزيع حجم الحبيبات والعلاقات المتبادلة الطوبوغرافية أثناء نضوج أوستوالد: محاكاة نموذج مونت كارلو بوتس

عملية معظم المواد متعددة البلورات مثل السيراميك تتكلس بواسطة سائل أثناء معالجة السيراميك. فعلى سبيل المثال يستخدم كربيد التتجستن في أدوات القطع. في عملية تلبد السائل يعتمد تركيب الحبيبات على عملية نضوج أوستوالد. في هذا العمل تم توظيف نموذج مونت كارلو بوتس لمحاكاة نضوج أوستوالد في خليط من الصلب والسائل. على أساس المحاكاة الحاسوبية تم تحليل توزيع حجم الحبيبات والارتباطات الطوبوغرافية لسلسلة من الحجم النسبية للحبيبات الصلبة تتراوح بين 40% - 90%.

ولقد وجد أنه بعد فترة طويلة في الحالة شبه الثابتة يبقى توزيع حجم الحبيبات والتوزيع الطوبوغرافي لجوانب الحبيبات ثابتا مع مرور الوقت. ويظهر كذلك أن توزيع حجم الحبيبات يمكن وصفه بشكل جيد للغاية باقتران التوزيع العادي. بينما عند الحجم النسبية العالية يكون توزيع حجم الحبيبات في اتفاق جيد مع الدالة التحليلية لتوزيع حجم الحبيبات القائمة على أساس نظرية متوسط المجال الإحصائية لنمو الحبيبات. وعلاوة على ذلك وجد أن توزيع حجم الحبيبات يعتمد على الحجم النسبي للحبيبات الصلبة وتصبح قيمة النهاية العظمى للمنحنى أعلى كلما زاد الحجم النسبي.

### Abstract

Practically most polycrystalline materials such as ceramics are sintered by liquid during processing; for example, tungsten carbide applied for cutting tools. In liquid sintering, grain structure is controlled by Ostwald ripening. In this work, the Monte Carlo Potts model is employed to simulate Ostwald ripening in solid-liquid mixture. Based on the computer simulation,

\* Physics Department \_ Al-Aqsa University \_ Gaza, Palestine.

\*\* Electrical Engineering Department \_ Islamic University \_ Gaza, Palestine.

## **Grain Size Distribution and topological ....**

the grain size distribution and the topological correlations were analyzed for a series of volume fraction of the solid grains varies between 40% - 90%.

It is found that after a long time within the quasi-stationary state, the scaled grain size distribution and the topological distribution of grain sides keep invariant with time. It is further shown that the scaled grain size distribution can be described very well with the normal distribution function. Whereas at high volume fractions, the scaled grain size distribution is in very good agreement with an analytical grain size distribution function based on a statistical mean-field theory of grain growth. Moreover, the grain size distribution is found to be dependent on the volume fraction of the solid grains. It becomes more peaked as the volume fraction increases.

### **I. Introduction**

Practically most engineering materials such as barium titanate electrical capacitors are processed using liquid phase sintering by dispersing solid grains in a liquid matrix. Sintering happens in a variety of temperatures and increases near the melting points. In liquid sintering, the solid grains dissolve in the liquid; therefore, the solid is wetted by the liquid producing capillary force, which attracts the grains (German *et al.*, 2009). The two-phase structure is unstable and undergo variation with time to reduce the interfacial energy between the solid grains and the liquid matrix. The interfacial energy is minimized by moving atoms from high interfacial curvature areas to low interfacial curvature through long-range diffusion. This process is named Ostwald ripening. As a result, the grain structure of the two-phase mixture varies with time (Voorhees, 1992). Thus, understanding grain structure during Ostwald ripening plays an important role in enhancing materials performance during industrial applications.

The Ostwald ripening is theoretically investigated by Lifshitz, Slyozov and Wagner (Lifshitz and Slyozov, 1961; Wagner, 1961) and their approach renowned LSW theory for very finite volume fraction. They first studied the evolution of one grain in a random population and next considered the continuity equation. Then, they derived formulae for the variation of the mean grain size with time and the grain size distribution function. They showed that the mean grain size increases proportionally to the cubic root of

time; moreover, the grain size distribution is time invariant in the self-similar regime.

Ardell (1972) extended LSW theory to consider the volume fraction of the solid grains. He projected that the grain growth law  $R \sim t^{1/3}$  is kept the same as LSW theory. However, the grain size distribution widens swiftly at small values of volume fractions,  $\phi$  and becomes duplicate to the grain size distribution developed by Wagner for interface-controlled coarsening in the limit  $\phi=1$ . While the grain size distribution is similar to the one predicted by the diffusion-controlled LSW close to zero volume fraction.

Voorhees and Glicksman (1984) considered Ostwald ripening using numerical methods based on multi-particle diffusion solution. They found that the grain structure evolved to indistinguishable steady distributions, which depend on the volume fraction of the growing phase. These time invariant distributions are dramatically different from LSW distribution; in addition, they become wider and further symmetric as the volume fraction increases.

Marqusee and Ross (1984) investigated Ostwald ripening for finite volume fractions using a multiple scattering approach. They showed that the grain size distribution skewed to the right at higher volume fractions. However, Fang et al. (1992) predicted grain size distribution skewed to lower sizes by employing a numerical method based on finite differences to simulate Ostwald ripening statistically.

Hillert (1965) was first considered grain growth classical theory based on LSW approach. Research efforts followed (Atkinson, 1988; Mullins, 1998; Streitenberger, 1998; Zöllner and Streitenberger, 2006) to develop LSW approach for grain growth theory as well as the grain size distribution for topological correlations.

Streitenberger (2013) developed an analytical approach to understand the effect of volume fraction on grain growth controlled by long-range diffusion. Based on the LSW technique, he derived an analytical grain size distribution function in terms of the scaled grain size variable.

The purpose of this work is to implement computer simulations based on Monte Carlo Potts model to study grain size distribution of grain growth controlled by long-range volume diffusion in solid-liquid mixture. The simulations will be performed for a broad range of solid grain fractions changes between 40%-90%. The simulated grain size distributions will be compared with grain size distribution derived by the authors in

## Grain Size Distribution and topological ....

(Streitenberger, 1998; Zöllner and Streitenberger, 2006; 2010) together with the normal Gaussian distribution function. Another important property of the microstructure is the topological correlations, which will be established by considering the relationship between the number of sides per grain and the distribution of sides per grain.

### II. Theoretical grain size distribution and topology

The grain structure during Ostwald ripening can be described by two geometric features: the average grain size of the ensemble and the grain size distribution. During Ostwald ripening, the atoms move from small gains to large grains by long-range volume diffusion. This process continues until the small grains shrink and vanish while large grains grow in size. Therefore, the number of grains decline and the grains grow in size. Simultaneously the grain structure evolves to a quasi-stationary state, which shows self-similarity. This implies that all grain size distribution functions in the self-similar regime end to a particular stationary grain size distribution function.

In the quasi-stationary state, the set of grain size distribution function can be represented by the following formula,

$$F(R,t)=g(t).f(x) \quad (1)$$

where the stationary grain size distribution function  $f(x)$  varies only with variation of the relative grain size,  $x=R/\langle R \rangle$ , and the only time dependent function  $g(t)=N/\langle R \rangle$ . The time development of the mean grain size obeys the parabolic growth law

$$\langle R \rangle^3 = \langle R \rangle_0^3 + kt \quad (2)$$

where  $k$  is the growth factor. The area of each grain is equal to the number of Monte Carlo units representing the grain, where a Monte Carlo unit can be considered as a square with a length equal to the lattice spacing. Knowing that the total area  $A$  of the considered grain structure is conserved, the total number of grains can be given by

$$N = \frac{A}{\langle A \rangle} = \frac{A}{4\pi \langle R^2 \rangle} = \frac{A}{4\pi \langle x^2 \rangle \langle R \rangle^2} \quad (3)$$

Substituting  $\langle R \rangle$  from equation (2) into equation (3) produces the fitting formula

$$N(t) = (kt + \langle R \rangle_0^3)^{-2/3} \quad (4)$$

The LSW approach is the basis of the classical theory of Ostwald ripening. In LSW approach, the relation between the growth law and the grain size distribution function through the continuity equation has been derived under the scaling assumption in equation (1). The grain size distribution function derived by LSW approach for volume diffusion controlled Ostwald ripening is given by the following expression (Lifshitz and Slyozov, 1961; Wagner, 1961),

$$f(x) = \frac{3^3 x^2 \exp(1)}{2^{5/3} (3+x)^{7/3} (3/2-x)^{11/3}} \exp\left(-\left(1-\frac{2}{3}x\right)^{-1}\right), \text{ for } x \leq 3/2 \quad (5)$$

Streitenberger 's approach of grain growth (Zöllner and Streitenberger, 2006 ) is derived based on a statistical mean-field theory producing the following scaled grain size distribution function,

$$f(x) = ax_0^a \exp(a) \frac{x}{(x_0-x)^{a+2}} \exp\left(\frac{-ax_0}{(x_0-x)}\right), \text{ for } 0 \leq x \leq x_0 \quad (6)$$

with the fitting parameter  $x_0$  given by

$$x_0 = \frac{a(x_0)^{a(x_0)-1}}{\exp(a(x_0))\Gamma(a(x_0)-1, a(x_0))}. \quad (7)$$

using the incomplete Gamma-function  $\Gamma(a-1, a)$  where  $a=a(x_0)$  is a parameter given implicitly in equation (7). This grain size distribution function is normalized and relates to the average grain size variation with time as  $t^{1/2}$ .

## Grain Size Distribution and topological ....

Another property of the microstructure is the topological correlations between the number of sides per grain and the distribution of sides per grain. Due to the grain growth process this correlation varies with time; however, within the quasi-stationary state the distribution of faces per grain keeps invariant with time. Next section is dedicated to present the simulation approach. Simulation results are given in section IV followed by conclusion in section V.

### III. Simulation approach

The Monte Carlo Potts model has been applied to study grain growth in one-phase systems (Anderson *et al.*, 1984; 1989; Song and Liu, 1998; Blikstein and Tschiptschin; 1999; Yu and Esche, 2003a; 2003b; Hui *et al.*, 2003; Huang *et al.*, 2006; Zöllner and Streitenberger, 2008), two-phase systems (Tikare and Gawlez, 1998; German *et al.*, 2009; El-Khozondar *et al.*, 2006; El-Khozondar, 2004; Solomatov *et al.*, 2002; El-Khozondar, 2015; El-Khozondar *et al.*, 2014) and three-phase systems (El-Khozondar, 2009). In the present work, the Monte Carlo Potts model adapted by Solomatov *et al.* (2002) to study grain growth in two-phase polycrystalline materials was modified to study Ostwald ripening in solid-liquid materials.

The microstructure is mapped on to a two-dimensional discrete square lattice with periodic boundary conditions. Each lattice point in the simulation is named a site, which characterizes an individual orientation of the crystalline lattice. In the presented two-dimensional simulations, the lattice size is  $400 \times 400$ . Thus, the total number of lattice sites is  $N = 160,000$ . The smallest time unit of the simulations is named one Monte Carlo step (MCS) and represents  $N$  orientation attempts.

The initial microstructure were created by occupying in a probabilistic way the lattice with the volume fraction of phase A and phase B as needed. The A-sites are the grains of the solid phase and the B-sites are the liquid matrix. Each lattice point of phase A is assigned positive numbers selected randomly from different orientations between 1 and  $q$  where  $q$  is the total number of orientations and has the value of  $q=100$ . However, each lattice point of phase B is given a negative number which represent one state with value  $q=-1$ .

A grain is a cluster of sites with the same orientation. Therefore, a grain boundary is defined as a separation edge between grains with different orientations. The interfacial energy between solid and liquid is  $E_{ab}$ . The grain boundary between grains with different orientations is  $E_{aa}$  in the solid phase. In the liquid phase, the interfacial energy is absent ( $E_{bb}=0$ ) because all sites have the same orientation. The values of the interfacial energies are chosen such that the value of  $E_{aa}$  are greater than the value of  $E_{ab}$ . Ostwald ripening is simulated using  $E_{aa}=2.5$  and  $E_{ab}=1$ .

The microstructure changes by Ostwald ripening is simulated as follows. In the first step, a site randomly selected and its neighbor is chosen in a probabilistic way from its eight nearest neighbors. If the two sites are from different phases, then the A-site has an orientation  $q_i$  and the current state of the lattice is called old state ( $E_i$ ). In the second step, both A-site and B-site are permitted to exchange their orientation to generate a new state ( $E_j$ ). In the third step, the energy difference ( $\Delta E = E_j - E_i$ ) of the two sites between new state  $E_j$  and old state  $E_i$  is calculated. The energy of a site is given by the following equation,

$$E_i = \sum_{i=1}^8 [1 - \delta(q_i - q_j)] \quad (8)$$

Each pair of nearest neighbors adds unit to the system energy if they have different orientations and zero otherwise. The new orientation of the two sites is selected by the next rule. If  $\Delta E$  is less than zero, the exchange is accepted. However, if  $\Delta E$  is greater than zero, the following exchange probability function is used.

$$P = \exp\left(-\frac{\Delta E}{kT}\right) \quad (9)$$

where  $T$  is the temperature and  $k$  is the Boltzman constant. The temperature has the value of  $T=1.3$ . After each attempt, the time is incremented by  $1/N$  MCS.

## Grain Size Distribution and topological ....

### IV. Simulation Results

In this paper, the Monte Carlo Potts model has been implemented in two dimensions based on the original works of Solomatov et al. (2002). An initial microstructure has been mapped onto a square lattice with eight nearest neighbors and periodic boundary condition. The grain microstructure resulted from grain growth can be described by geometrical features and topological features. The geometrical features are grain size and grain size distribution. The topological feature is the distribution of the number of sides,  $f(n)$  vs. the number of sides,  $n$ .

It has been shown in previous work (El-Khozondar, 2015) that the grain growth during Ostwald ripening is controlled by long-range diffusion and the average grain size follows the power growth law Equation (2). As the growth continues, the average grain size increases and the number of grains drops.

Figure 1 exhibits the number of grains as a function of time for a broad range of solid fractions varies between 40%-90%. It can be seen from Figure 1 that the number of grains declines (solid line) following the self-similar regime Equation 4 having the value of exponent from numeric fit (dashed line) equals to  $-2/3$ . It can further be seen from Figure 1 that the self-similar regime is approached at different aging times varies with the volume fraction of the solid grains. The self-similar regime is approached at  $t=9000$  MCS for volume fraction equals to 40%. At volume fraction equals to 50%, the self-similar regime is reached at  $t=7000$  MCS. While the self-similar regime is achieved at  $t=5000$  MCS for both volume fractions having values of 60% and 70%. Whereas the the self-similar regime is attained at  $t=2000$  MCS for volume fraction equals to 80%. When the volume fraction has a value equal to 90%, the self-similar regime is arrived at  $t=1000$  MCS. This means that the self-similar regime is approached at earlier times as the



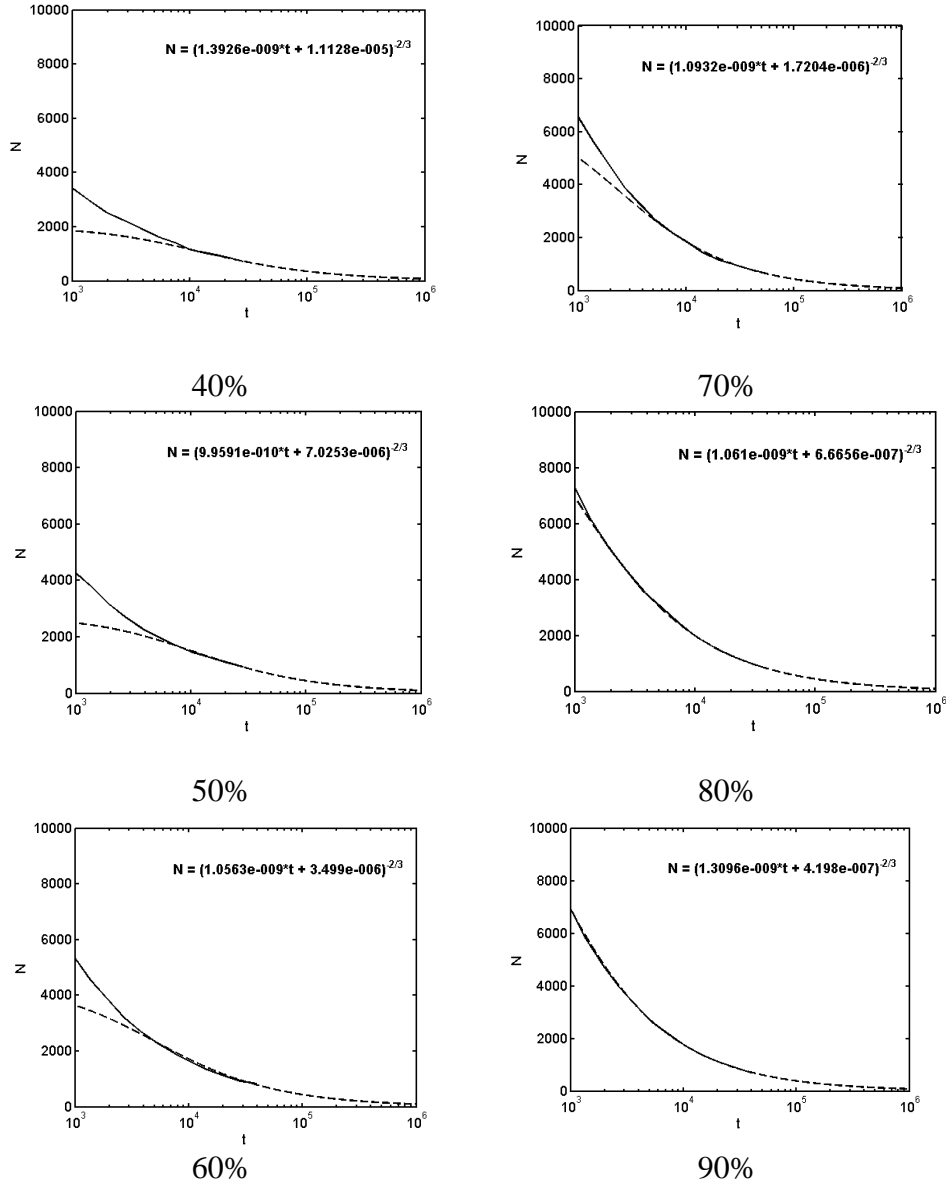


Figure 1: Time dependence of the number of grains (N) for different volume fraction of the solid grains (solid line) fitted with equation (4) (dashed line). The volume fraction of the solid grains (phase A) ranges between 40 % - 90% as indicated.

## Grain Size Distribution and topological ....

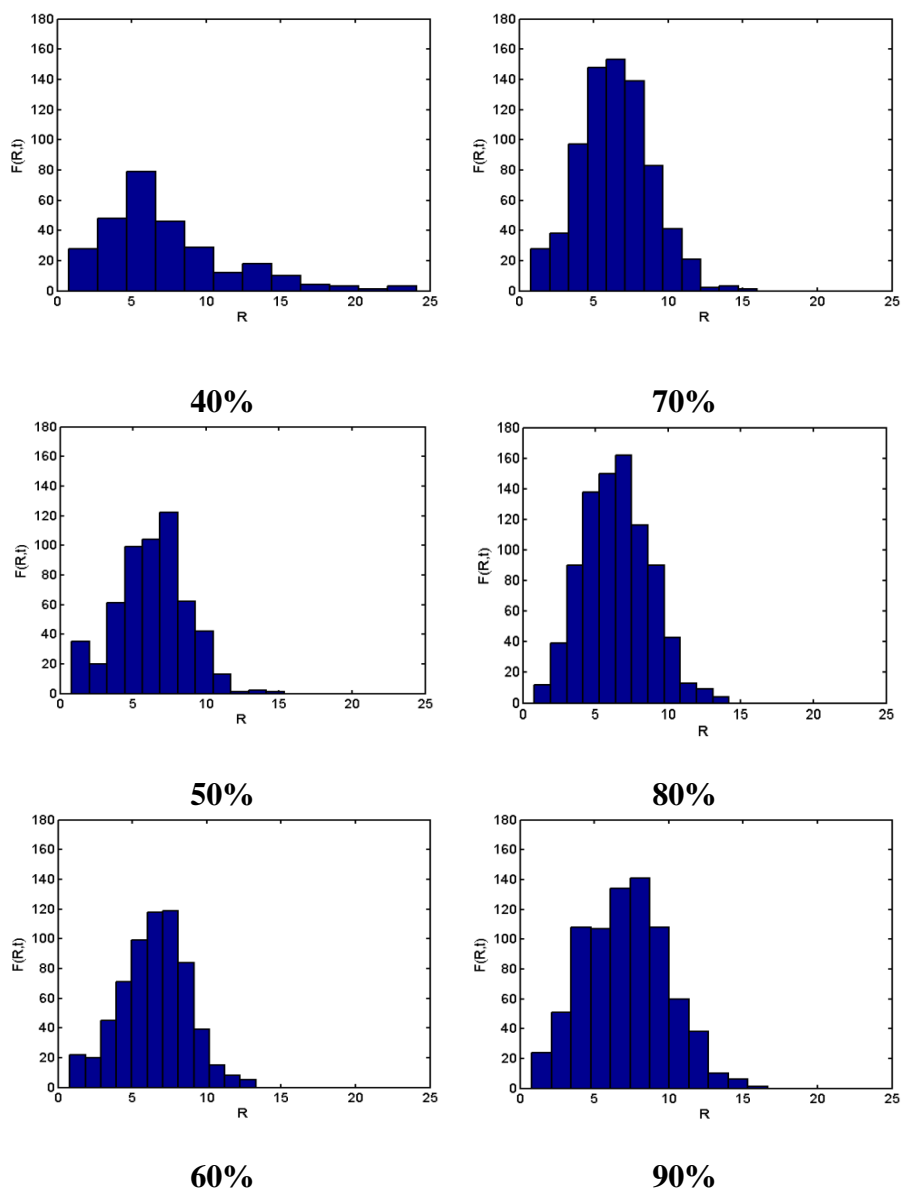


Figure 2: Grain size distribution as a function of the average grain size,  $R$ , for various volume fractions of the solid grains at  $t = 28348$  MCS. The volume fraction of the solid grains (phase A) varies between 40% - 90% as indicated.

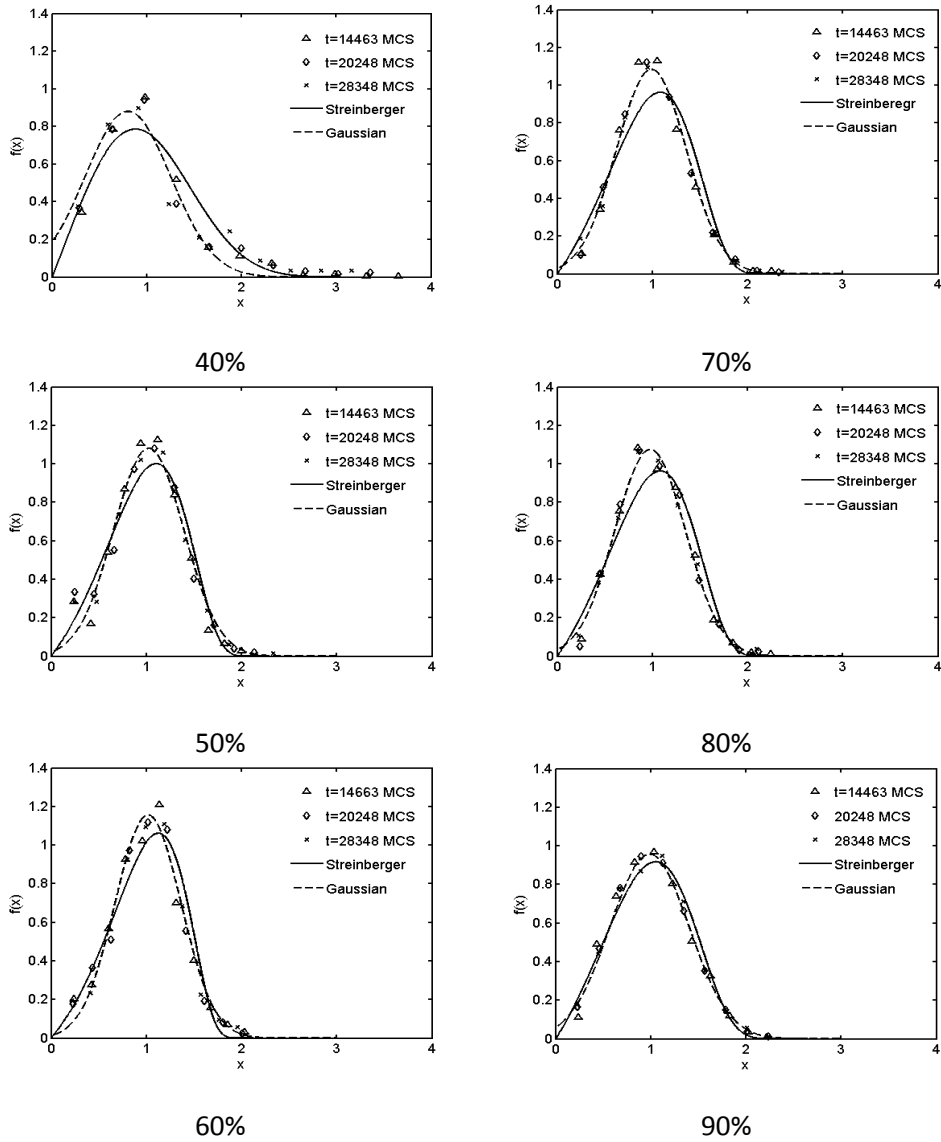


Figure 3: Dependence of scaled grain size distribution  $f(x)$  on solid fractions for three time steps, comparing with Equation (3) together with the normal Gaussian distribution function. The three time steps are 14463, 20248, 28348 MCS. The volume fraction differs between 40%-90% as indicated.

## Grain Size Distribution and topological ....

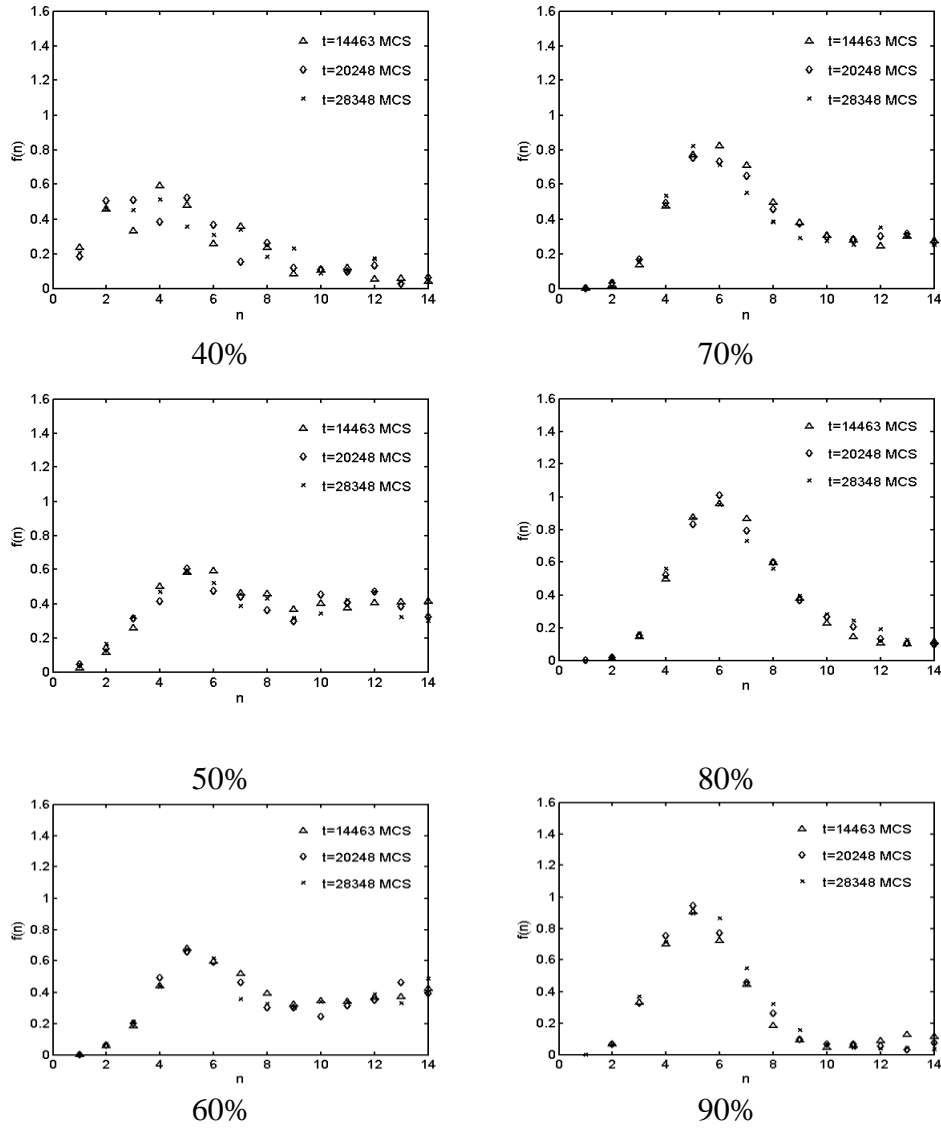


Figure 4: Variation of the distribution of the number of sides with volume fractions for three time steps. The three time steps are 14463, 20248, 28348 MCS. The volume fraction changes between 40%-90% as indicated. However, the self-similar regime is approached later as the volume fraction of the solid grains decreases.

When the self-similar regime is attained, the grain size distribution  $F(R,t)$  is described by Equation (1). Consequently, the scaled grain size distribution  $f(x)$  ends to an indistinguishable stationary grain size distribution.

Figure 2 displays the simulated grain size distribution  $F(R,t)$  at  $t= 28348$  MCS for different volume fractions vary between 40%-90%. The total sum of each interval multiplied by the interval width gives the total number of grains at this time step as specified in Figure 1. It can be noticed that the size distribution is more peaked at higher volume fractions of solid grains and skewed to smaller grains for solid fraction equal to 40%.

The quasi-stationary state of grain growth by Ostwald ripening is presented in Figure 3 by plotting the scaled grain size distribution at three variant time steps for a range of solid fractions varies between 40%-90%. It can be noticed that the size distributions in the quasi-stationary state are indistinguishable from each other. In addition, the simulated size distribution within the quasi-stationary state can be described very well by the normal distribution function. Comparing with the analytical distribution function Equation 6, it can be seen that the simulated size distribution within the quasi-stationary state is in excellent agreement with the analytical distribution function at high solid fraction with value equal to 90%. For solid fractions varies between 40%-80% the simulated size distributions within the quasi-stationary state are in very good agreement with the analytical distribution function but with higher peaks. The simulated size distributions within the quasi-stationary state are symmetric and peaked at  $x=1$  for the broad range of solid fractions varies between 40%-90%. However, the simulated size distributions within the quasi-stationary state is skewed to smaller grains at volume fraction of solid grains equal to 40%.

Additional significant property of the grain structure is the topological correlation between the frequency of the number of sides per grain  $f(n)$  and the number of sides per grain ( $n$ ). Figure 4 shows the dependence of the distribution of the number of sides on volume fraction for three different time steps. The three time steps are 14463, 20248, 28348 MCS. It can be observed that the distribution of the number of grain sides has a behavior

## **Grain Size Distribution and topological ....**

similar to the grain size distributions. This means that the distribution of the number of grain sides have self-similarity in the quasi-stationary state.

### **V. Conclusion**

Computer simulations based on Monte Carlo Potts model has been employed to investigate grain structure controlled by Ostwald ripening. The grain structure changes during Ostwald ripening and eventually approaches the quasi-stationary state. It is noticed that the quasi-stationary state is approached at different aging times depending on the case of the solid fraction. It has also been shown that within the quasi-stationary state, the scaled grain size distribution functions end to an identical self-similar time independent grain size distribution function.

The simulated distribution function is found to be characterized very well by the normal distribution function; moreover, the simulated size distributions within the quasi-stationary state are in excellent agreement with the analytical distribution function at higher solid fraction. Additionally, the simulated size distributions within the quasi-stationary state is skewed to smaller grains at lower solid fraction equal to 40% whereas symmetric at higher solid fractions.

Another property of grain structure is the topological correlation between the frequency of the number of sides per grain and the sides per grain. It has been shown that the distribution of sides per grain is time invariant and exhibits self-similarity in the quasi-stationary state as shown for grain size distribution.

### **References:**

1. Anderson M.P., Grest G.S., Srolovitz D.J., 1989: Computer simulation of grain growth in three dimensions, *Phil. Mag.*, 59B, 293-329.
2. Anderson M.P., Srolovitz D.J., Grest G.S., and Sahni P.S., 1984: Computer simulation of grain growth-I. Kinetics, *Acta Metall.*, 32, 783-791.
3. Ardell A.J. 1972: The effect of volume fraction on particle coarsening: Theoretical considerations, *Acta Metall.*, 20, 61-71.

4. Atkinson H.V., 1988: Theories of normal grain growth in pure single phase systems, *Acta Metall.*, 36(3), 469-491.
5. Blikstein P. and Tschiptschin A. P., 1999: Monte Carlo simulation of grain growth, *Materials Research*, 2, 133-137.
6. El-Khozondar R. and El-Khozondar H., 2004: Numerical simulations of coarsening of lamellar structures: applications to metallic alloys, *Egypt. J. Solids*, 27(2), 189-199.
7. El-Khozondar R. and El-Khozondar H., 2009: Numerical modeling of microstructural evolution in three-phase polycrystalline materials, *Arab. J. Sci. Eng.*, 34(1A), 241-252.
8. El-Khozondar R. and El-Khozondar H., 2015: Monte Carlo Potts simulation of grain growth of solid grains dispersed in a liquid matrix, *Journal of Engineering Research and Technology*, 2(1), 7-14.
9. El-Khozondar R., El-Khozondar H., Gottstein G., Rollet A., 2006: Microstructural Simulation of Grain Growth in Two-phase Polycrystalline Materials, *Egypt. J. Solids*, 29(1), 35-47.
10. El-Khozondar R., Zöllner D., and Kassner K., 2014: Numerical simulation of grain size distribution in two-phase polycrystalline materials, *International Journal of Materials Science and Applications*, 3(6), 381-390.
11. Fang Z., Patterson B.R., Turner M.E. 1992: Influence of particle size distribution on coarsening, *Acta Metall. Mater.*, 40(4), 713-722.
12. German R.M., Suri P., Park S.J. 2009: Review: liquid phase sintering, *J. Mater. Sci.*, 44, 1–39.
13. Hillert M., 1965: On the theory of normal and abnormal grain growth. *Acta Metall.*, 13, 227-238.
14. Hui L., Guanghou W., Feng D., Xiufang B., and Pederiva F., 2003: Monte Carlo simulation of three-dimensional polycrystalline material, *Mater. Sci. Eng., A*, 357, 153-158.

## **Grain Size Distribution and topological ....**

15. Lifshitz I.M. and Slyozov V.V. 1961: The kinetics of precipitation from supersaturated solid solution, *J. Phys. Chem. Solids*, 19, 35-50.
16. Marqusee J. A. and Ross J. 1984: Theory of Ostwald ripening: Competitive growth and its dependence on volume fraction, *J. chem. Phys.*, 80(1), 536-543.
17. Ming Huang C., Joanne C.L., Patnaik B.S.V., and Jayaganthan R., 2006: Monte Carlo simulation of grain growth in polycrystalline materials, *Appl. Surf. Sci.*, 252, 3997-4002.
18. Mullins W.W., 1998: Grain growth of uniform boundaries with scaling, *Acta mater.*, 46(17), 6219-6226.
19. Solomatov V.S., El-Khozondar R., and Tikare V., 2002: Grain size in the lower mantle: constraints from numerical modeling of grain growth in two-phase systems, *Phys. Earth. Planet. Inter.*, 129, 265-282.
20. Song X. and Liu G., 1998: A simple and efficient three-dimensional Monte Carlo simulation of grain growth, *Scr. Mater.*, 38, 1691-1696.
21. Streitenberger P., 1998: Generalized Lifshitz-Slyozov theory of grain and particle coarsening for arbitrary cut-off parameter, *Scr. Mater.*, 39, 1719-1724.
22. Streitenberger P., 2013: Analytical description of phase coarsening at high volume fractions, *Acta Metall.*, 61, 5026-5035.
23. Tikare V. and Gawlez J.D., 1998: Applications of the Potts model to simulation of Ostwald ripening, *J. Am. Ceramic Soc.*, 81, 485-491.
24. Voorhees P.W. 1992: Ostwald ripening of two-phase mixtures, *Ann. Rev. Mater. Sci.*, 22, 197-215.
25. Voorhees P.W. and Glicksman M.E. 1984: Solution to the multi-particle diffusion problem with applications to Ostwald ripening-II. Computer Simulations, *Acta Metall.*, 32(11), 2013-2030.
26. Wagner C. 1961: Theorie der alterung von niederschlägen durch unlösen, *Elektrochem.*, 65, 581-591.



27. Yu Q. and Esche S.K., 2003a: A Monte Carlo algorithm for single phase normal grain growth with improved accuracy and efficiency, *Comput. Mater. Sci.*, 27, 259-270.
28. Yu Q. and Esche S.K., 2003b: Three-dimensional grain growth modeling with a Monte Carlo algorithm, *Mater. Lett.*, 57, 4622-4626.
29. Zöllner D. and Streitenberger P., 2010: Grain size distributions in normal grain growth, *Practical Metallography/Praktische Metallographie*, 47, 618-639.
30. Zöllner D. and Streitenberger P., 2008: Monte Carlo Simulation of Normal Grain Growth in Three Dimensions, *Mater. Sci. Forum*, 567, 81-84.
31. Zöllner D. and Streitenberger P., 2006: Three-dimensional normal grain growth: Monte Carlo Potts model simulation and analytical mean field theory, *Scr. Mater.*, 54, 1697-1702.